Data-enhanced learning compensation for linear predictive control of nonlinear chemical processes

Yuanqiang Zhou * **Furong Gao** **

* *Department of Chemical and Biological Engineering, Hong Kong University of Science and Technology, Kowloon, Hong Kong*
** *Department of Chemical and Biological Engineering, Hong Kong University of Science and Technology, Kowloon, Hong Kong and Guangzhou HKUST Fok Ying Tung Research Institute, Guangzhou 511458, China*
(e-mail: kefgao@ust.hk)

Abstract: In chemical processes, nonlinearities, uncertainties, and constraints have resulted in much more complex optimization problems, since optimization algorithms depend on model characteristics. Optimization success for chemical processes requires a proper combination of the optimization technique and the model that is appropriate. In this paper, we propose a data-enhanced learning compensation method for linear predictive control of nonlinear chemical processes. By using more reliable data to increase the accuracy of the model, optimizing performance can be greatly enhanced. Our method can be used in situations where engineering constraints must be met by a system with dynamics not well understood or nonlinearities that make previous control methods ineffective. Finally, a practical example of the CSTR is provided to demonstrate the efficacy of the proposed methods.

Keywords: Model predictive control, constrained systems, nonlinear control systems, data-driven control, process control, optimization.

1. INTRODUCTION

Over the past 20 years, the chemical industry has undergone significant change due to higher energy costs, stricter environmental regulations, and increased global competition for pricing and quality. In order to deal with these issues, optimization is one of the most important engineering tools (Edgar et al. (2001)). To reduce costs and meet constraints, plant designs and operating procedures have been modified, with a focus on improving efficiency and increasing profitability. Optimal operating conditions can be implemented via increased automation at the process level. However, the constraints, nonlinearities, and uncertainties of chemical processes have greatly increased the size and complexity of the optimization problems.

Chemical processes always involve nonlinear dynamics and constraints. Therefore, constrained optimization is more suitable for controlling chemical processes. Usually, the optimal operating point of a plant lies at the intersection of constraints. To achieve economic objectives of a process, the real-time modeling of nonlinear behaviors and the constraints handling become critical issues for any successful controller (Zhou et al. (2022c)). Prett and García (2013) point out that model predictive control (MPC) is the only way to handle constraints effectively. MPC and linear quadratic regulation (LQR) are popular techniques because of their theoretical foundations and their robustness and stability guarantees. However, many formulations use linear time-invariant (LTI) approximations of the dynamics of the system (Mayne (2014)). In order to enhance closed-loop performance and maintain these robustness and stability guarantees, data science and machine learning can be incorporated into constrained optimal control problems.

⋆ This work was supported in part by the Ministry of Science and Technology of China (SQ2019YFB170029), the Hong Kong Research Grant Council (16208520), the Guangdong scientific and technological project (202002030323), and the Foshan-HKUST Project (FSUST19-FYTRI01).

In recent years, data science and machine learning have been increasingly used in chemical processes (Qin and Dong (2020)) since modern information technology allows us to collect huge amounts of data, such as historical data from previous measurements and real-time data during process runs. It would be extremely helpful if we could use those online or offline process data to predict and assess system states, make decisions, and perform real-time optimization (Zhou et al. (2022b,a)). Using long-short-term memory (LSTM) networks to train the process model, Wu et al. (2021) focused on machine learning modeling and MPC of nonlinear processes. In order to identify richer models of the system, Aswani et al. (2013) used statistical identification tools and developed a learning controller using MPC formulation. Utilizing historical inputs and/or outputs data, Lu et al. (2019) examined various levels of data-driven learning mechanisms to process control with constraints. Results above illustrate that data-driven learning (always including optimization) is a superior method for handling nonlinearities and/or constraints in process control. In light of this, we are investigating the data-driven learning method for chemical processes.

In this paper, we explore how data-driven learning can be incorporated into constrained optimal control for chemical processes. With the advancement of optimization algorithms, the modeling step usually presents more choices and challenges than the optimization technique (Zhou (2012); Yang et al. (2016)). Hewing et al. (2020) categorized the research on learning-based MPC, i.e., integrating or combining MPC with learning methods. Thus, we propose a data-enhanced learning compensation method for linear predictive control of nonlinear chemical processes. We demonstrate that by utilizing more efficient data to improve the accuracy of the model, the control performance can be enhanced, and the convergence rate can be increased. The flexibility of our design allows it to handle situations in which engineering constraints have to be met by a system exhibiting dynamics not well understood or nonlinear-

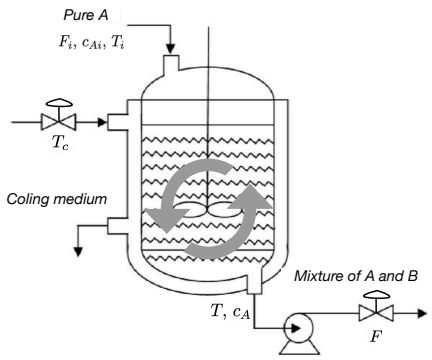

Fig. 1. A simplified illustration of the CSTR

ities that make traditional control methods ineffective. Finally, through numerical experiments for the continuous stirred-tank reactor (CSTR) systems that are ubiquitous in the chemical industry, we demonstrate that the data-enhanced learning MPC is more efficient than LQR and (robust) MPC.

Notations. For vector x, x^T denotes its transpose. For matrix $A \in \mathbb{R}^{n\times n}$, $A \succ 0$ or $A \succeq 0$ means that A is positive definite or semi-positive definite. Given two sets A and B, set addition $A \oplus B \triangleq \{a+b | a \in A, b \in B\}$; set subtraction $A \ominus B \triangleq \{a | a \oplus B \subseteq A\}$.

2. MOTIVATING EXAMPLE: A NONLINEAR CSTR

In chemical industry, the CSTR has many features similar to those found in other types of chemicals reactors, such as tubular reactors and packed bed reactors. Therefore, a CSTR model makes it easy to demonstrate how modeling principles apply to other chemical reactors (Seborg et al. (2010)). Here we consider an irreversible liquid-phase chemical reaction in a CSTR shown in Fig. 1, in which chemical species A reacts in the vessel to form chemical species B, that is, $A \rightarrow B$. As shown in Fig. 1, the inlet stream contains pure component A with a molar concentration, c_A. By removing the heat that is released during the exothermic reaction, a cooling coil is used to maintain the reaction mixture at its operating temperature. Detailed modeling for such a CSTR system is described in Seborg et al. (2010), where mass and energy balances result in a nonlinear state-space model given by

$$\frac{dc_A}{dt} = \frac{F\left(c_{Ai} - c_A\right)}{V} - k_0 \exp\left(-\frac{E}{RT}\right) c_A \tag{1a}$$

$$\frac{dT}{dt} = \frac{F\left(T_i - T\right)}{V} - \frac{\Delta H_R}{\rho C_p} k_0 \exp\left(-\frac{E}{RT}\right) c_A + \frac{UA}{V\rho C_p}\left(T_c - T\right) \tag{1b}$$

where the state variables are the molar concentration of species A, denoted as c_A, and the reactor temperature, denoted as T; the manipulated variable is the coolant jacket temperature T_c. The model parameters in nominal conditions are reported in Table A.1. Moreover, the chemical reactor is designed to operate under steady-state conditions:

$$c^s = 0.878 \text{ mol/L}, T^s = 324.5 \text{ K}, T_c^s = 300 \text{ K} \tag{2}$$

Additionally, we consider the constraints on state and manipulated variables for the CSTR system given by (1). These constraints (Zhou et al. (2020)) are set as follows:

$$130 \text{ K} < T < 454 \text{ K}, \quad 60 \text{ K} < T_c < 540 \text{ K} \tag{3a}$$

$$0.4386 \text{ mol/L} < c_A < 1.3159 \text{ mol/L}. \tag{3b}$$

Next, we outline all the assumptions that were used to formulate the dynamics (1). For mass balance equation given by (1a), the following three assumptions are used: i) the CSTR is perfectly mixed; ii) the mass densities of the feed and product streams are equal and constant; iii) the liquid volume in the reactor is kept constant. For energy balance equation given by (1b), assumptions used are as follows: i) the coolant temperatures and the cooling coil walls have negligible thermal capacitances compared with liquid temperatures; ii) all of the coolant is at the same temperature as T_c; iii) the rate of heat transfer from the reactor contents to the coolant is given by $UA(T_c - T)$, where U is the overall heat transfer coefficient and A is the area of heat transfer. U and A are assumed to be constants; iv) the enthalpy change associated with mixing the feed with the liquid in the tank is negligible compared with the enthalpy change for the chemical reaction; that is, the heat of mixing is negligible compared to the heat of reaction; v) shaft work and ambient heat losses can be neglected. Using all the above assumptions, we define normalized and dimensionless variables x and u as $x = \left[x_1^{\mathrm{T}}, x_2^{\mathrm{T}}\right]^{\mathrm{T}}$ and $u = (T_c - T_c^s)/T_c^s$ with $x_1 = (c_A - c^s)/c^s$ and $x_2 = (T - T^s)/T^s$. Next, to simplify the model given by (1), we use the nominal values for the parameters shown in Table A.1 and obtain the nonlinear process of the CSTR as follows:

$$\frac{dx_1}{dt} = -x_1 + 0.1399 - 7.2 \times 10^{10}(x_1 + 1) \exp\left(\frac{-26.9666}{x_2 + 1}\right) \tag{4a}$$

$$\frac{dx_2}{dt} = -3.0921 x_2 + 1.9342 u - 0.0791 + 4.0724 \times 10^{10}(x_1 + 1) \exp\left(\frac{-26.9666}{x_2 + 1}\right) \tag{4b}$$

As stated before, the model given by (4) was based on a lot of assumptions. This makes it difficult for the model to capture uncertainties inherent to the real plant, such as unmodeled dynamics and uncertainty in parameter values. Thus, it is best to use historical process data to help us build real-time models and perform optimizations in real-time. To accomplish this, we examine how historical data can be used to optimize control performance during controller design for the CSTR system illustrated in Fig. 1. Since all the historical process data, such as the inputs and states, are available, we use the notations $\mathbb{I}$ and $\mathbb{O}$ to indicate the input and state data sets; that is, $\mathbb{I} \triangleq \{u_0, u_1, \ldots, u_K\}$ and $\mathbb{O} \triangleq \{x_0, x_1, \ldots, x_K\}$. It is important to note that the nonlinear model given by (4) is continuously differentiable and it is used to simulate plant responses and perform verification in the presence of uncertainties, even when some advanced linear control system design techniques are used in the next section.

3. CONTROLLER DESIGNS

In this work, we consider that only a linear model of the nonlinear chemical process around the operating point is available for controller design, and that linear model is described by

$$x(t+1) = Ax(t) + Bu(t) \tag{5}$$

in which t is the sampling time and $x(t) \in \mathbb{R}^n$ and $u(t) \in \mathbb{R}^m$ denote the state and input, respectively, with n and m representing dimensions. The matrix pair (A, B) is assumed to be controllable. The following sections will provide several controllers for the process, highlighting our main results.

3.1 LQR

In LQR controller, the optimization relies on the minimization of quadratic cost function (Olalla et al. (2009)). In most cases, LQR controllers provide superior performance without complicated algorithms and additional computational analysis. Besides, the LQR controller is simple, easy to implement, and

has a lower memory capacity (Ogata (2010)). In this subsection, we focus on LQR formulation for the system. Generally, the LQR controller is designed with the from of $u(t) = Kx(t)$, where $K \in \mathbb{R}^{m\times n}$ is a feedback control gain that is to be determined by optimizing the performance measure $J(x(t),u(t)) = \sum_{t=0}^{\infty} x^{\mathrm{T}}(t)Qx(t)+u^{\mathrm{T}}(t)Ru(t)$, where $Q \succeq 0$ and $R \succ 0$ are symmetric sign-definite weighting matrices. Thus, the LQR formulation for (5) is given by

$$\min_{u(t)} \; J(x(t),u(t)), \quad \text{s.t.} \quad (5) \tag{6a}$$

The complete LMI formulation of the problem given by (6) can refer to Olalla et al. (2009). Following Lewis et al. (2012), the unique solution to the LQR problem (6) is given by

$$u^{\star}(t) = Kx(t) \in \mathbb{R}^m \tag{7a}$$

where $K = -(R+B^{\mathrm{T}}PB)^{-1}B^{\mathrm{T}}PA$ and $P = Q+A^{\mathrm{T}}PA-A^{\mathrm{T}}PB(R+B^{\mathrm{T}}PB)^{-1}B^{\mathrm{T}}PA$. Note that the LQR is capable of achieving robust stability and stability despite model inaccuracies. However, it cannot take into account the constraints.

3.2 Tube-Based MPC

Since LQR cannot handle the constraints, we use an alternative MPC method. MPC is incredibly successful in the process industries because of its conceptual simplicity and its ability to deal with hard constraints(Qin and Badgwell (2003)). Several current developments in MPC are summarized in Mayne (2014). In this section, we develop a MPC method for the chemical system. For nominal MPC, we solve the optimal control problem (OCP) by disregarding all the disturbances. Because of the open-loop nature of OCP, we employ a simple parameterized local policy, termed tube-based MPC. Outlined by Chisci et al. (2001), tube-based MPC enforces the satisfaction of the constraints in solving OCP by keeping closed-loop trajectory inside tubes that satisfy the constraints.

For the system given by (5), we consider a parameterized local control policy as $u(t) = Kx(t)+\zeta(t)$, where K is the same as we used in (7). In this case, for (5), we obtain the uncertain term as $g(x(t),u(t)) \triangleq f(x(t),u(t))-Ax(t)-Bu(t)$, where $f(\cdot,\cdot)$ denotes a discrete-time representation of the uncertain nonlinear process. Besides, we assume that, given two polytope constraint sets $\mathscr{X}$ and $\mathscr{U}$, $g(\cdot,\cdot)$ is bounded as $g(x(t),u(t)) \in \mathscr{W} \subset \mathbb{R}^n$, $\forall x \in \mathscr{X}$, $u \in \mathscr{U}$. To ensure stability (Rakovic et al. (2012)), we need a control invariant set $\Omega \subset \mathbb{R}^n$ which resides the state at the end of each prediction horizon t, i.e., $x(t+N) \in \Omega$, where N denotes the prediction horizon. To enforce satisfaction of the constraints, we should have $\Omega \subset \{x : x \in \mathscr{X}, Kx \in \mathscr{U}\}$. For disturbance invariance, we should keep $(A+BK)\Omega \oplus \mathscr{W} \subset \Omega$. Methods for computing positively invariant outer approximations of Ω are given in Rakovic et al. (2005). To decrease conservatism and improve robustness, we use different disturbance tubes $\mathscr{R}_k$ for every prediction step, which satisfy

$$\mathscr{R}_0 = \{0\}, \quad \mathscr{R}_k = \oplus_{j=0}^{k-1}(A+BK)^k\mathscr{W}, \quad k = 1,2,\ldots,N. \tag{8}$$

Finally, the tube-based MPC problem can be formulated as

$$\min_{\bar{u}(t)} \; J_F(\bar{x}(t),\bar{u}(t)) \tag{9a}$$

$$= \sum_{k=t}^{t+N-1} \bar{x}^{\mathrm{T}}(t)Q\bar{x}(t)+\bar{u}^{\mathrm{T}}(t)R\bar{u}(t)+\bar{x}^{\mathrm{T}}(t+N)P\bar{x}(t+N)$$

$$\text{s.t.} \quad \bar{x}(t+k+1) = A\bar{x}(t+k)+B\bar{u}(t+k),\ \bar{x}(t) = x(t) \tag{9b}$$

$$\bar{u}(t+k) = K\bar{x}(t+k)+\zeta(t+k) \tag{9c}$$

$$\bar{x}(t+k+1) \in \mathscr{X} \ominus \mathscr{R}_{k+1},\ \bar{x}(t+N) \in \Omega \ominus \mathscr{R}_N \tag{9d}$$

$$\bar{u}(t+k) \in \mathscr{U} \ominus (K\mathscr{R}_k),\ k = 0,1,\ldots,N-1 \tag{9e}$$

By solving of (9), we obtain that nominal control and state sequences $\{\zeta(t),\zeta(t+1),\ldots,\zeta(t+N-1)\}$, $\{\bar{x}(t+1),\bar{x}(t+2),\ldots,\bar{x}(t+N)\}$ satisfies $\bar{x}(t+k+1) = A\bar{x}(t+k)+B\bar{u}(t+k) = A_K\bar{x}(t+k)+\zeta(t+k)$, where $A_K \triangleq A+BK$. In this case, for the uncertain system given by

$$x(t+1) = Ax(t)+Bu(t)+g(x(t),u(t)) \tag{10}$$

with a given Ω, we obtain that control and state sequences $\{u(t),u(t+1),\ldots,u(t+N-1)\}$ and $\{x(t+1),x(t+2),\ldots,x(t+N)\}$ satisfy $x(t+k) \in \bar{x}(t+k)+\Omega$ and $u(t+k) \in \zeta(t+k)+K\Omega$ for all $k = 0,1,\ldots,N-1$. Because of (9d) and (9e), the actual trajectories will satisfy $x(t+k+1) \in \mathscr{X}$, $u(t+k) \in \mathscr{U}$, and $x(t+N) \in \Omega$. Finally, $x(t)$ will converge to Ω. This indicates that the set Ω is robustly stable for the system.

3.3 Main Results: Data-Enhanced Learning for Tube MPC

For the tube-based MPC given by (9), because of its use of a prediction model, it should be amenable to adaptive implementation and to the online tuning of the model. A disadvantage of tube-based MPC in (9) is that the dynamics of the system are constant at each time step. It seems wasteful since the historical process data are stored for each time step, as these data can provide adaptation to the model at each time step. Marafioti et al. (2014) proposed an approach to augment the input constraint set of MPC, guaranteeing that 'sufficient richness' of the periodic input signal properties or 'persistent excitation' can be fulfilled to ensure uniform identification of the model. It is our goal to use data-enhanced learning compensation when the 'persistent excitation' requirement is not met.

For the OCP (9), we note that the linear model attained from (9b) is used for predicting the response, along with the robustified constraints attained from (9d)-(9e), which assures robust constraint satisfaction. As additional data becomes available, we employ a separate model with adaptive approximations of the true (nonlinear) dynamics, which gives us more accurate input and output predictions to use in the objective function. To that end, we use a separate model with the form of

$$\tilde{x}(t+k+1) = A\tilde{x}(t+k)+B\tilde{u}(t+k)+\mathscr{O}_t(\tilde{x}(t+k),\tilde{u}(t+k)) \tag{11}$$

where $\mathscr{O}_t(\cdot,\cdot)$ is a data-enhanced learning function that is to be designed using historical process data. Since the function $\mathscr{O}_t(\cdot,\cdot)$ denotes a compensation term for prediction model (9b), which varies with time t and iteratively approximates the nonlinear portion of the system's dynamics, accuracy of the optimization can be increased with more data available.

Finally, the data-enhanced compensation for tube-based MPC solves the following OCP at each time step

$$\min_{\tilde{u}(t)} \; J_F(\tilde{x}(t),\tilde{u}(t)) \tag{12a}$$

$$= \sum_{k=t}^{t+N-1} \tilde{x}^{\mathrm{T}}(t)Q\tilde{x}(t)+\tilde{u}^{\mathrm{T}}(t)R\tilde{u}(t)+\tilde{x}^{\mathrm{T}}(t+N)P\tilde{x}(t+N)$$

$$\text{s.t.} \quad \tilde{x}(t+k+1) = A\tilde{x}(t+k)+B\tilde{u}(t+k) + \mathscr{O}_t(\tilde{x}(t+k),\tilde{u}(t+k)),\ \bar{x}(t) = x(t) \tag{12b}$$

$$\bar{x}(t+k+1) = A\bar{x}(t+k)+B\tilde{u}(t+k) \tag{12c}$$

$$\tilde{u}(t+k) = K\bar{x}(t+k)+\zeta(t+k) \tag{12d}$$

$$\bar{x}(t+k+1) \in \mathscr{X} \ominus \mathscr{R}_{k+1},\ \bar{x}(t+N) \in \Omega \ominus \mathscr{R}_N \tag{12e}$$

$$\tilde{u}(t+k) \in \mathscr{U} \ominus (K\mathscr{R}_k), \quad k = 0,1,\ldots,N-1. \tag{12f}$$

For this problem, (12c) is used to derive deterministic guarantees on the robustness and stability properties of the resulting closed-loop system, while (12b) is an adaptive model of the

system which learns the true underlying dynamics of the chemical system over time. Since the variable $\bar{x}$ is used in adaptive model (12b) with data compensation, thereby yielding more accurate predictions for the actual state trajectory. Choosing control inputs according to the learned (more accurate) dynamics (12b), yet subject to the robustness constraints on the model (12c), results in lower cost and higher performance, while also dropping the strict condition used in Marafioti et al. (2014).

Using (10), we obtain $g(x(t),u(t)) = f(x(t),u(t)) - Ax(t) - Bu(t)$. Thus, the main goal of $\mathscr{O}_t(\cdot,\cdot)$ in (12b) is to make that

$$\mathscr{O}_t(x(t),u(t)) \to g(x(t),u(t)) \tag{13}$$

as more data become available for compensation. With sufficiently rich data for approximating the nonlinear term, we would expect that the nonlinear system can be learned using (12b). Next, we shall discuss how we develop the data compensation method to ensure (13).

To save computational burden, we use the polynomial approximation to develop a parametric function, such that $\mathscr{O}_t(x(t),u(t))$ is a polynomial in $(x(t),u(t))$. Thus, we would like to find some positive integers r_1, r_2, such that

$$\mathscr{O}_t(x,u) = P_x^{\mathrm{T}} \overrightarrow{m}_{[0,r_1]}(x) + P_u^{\mathrm{T}} \overrightarrow{m}_{[0,r_2]}(u) \tag{14}$$

where $\overrightarrow{m}_{[0,r_1]}(x)$ and $\overrightarrow{m}_{[0,r_2]}(u)$ with two positive integer r_1 and r_2 denote the polynomials of the vector $x \in \mathbb{R}^n$ and $u \in \mathbb{R}^m$ with the order at least 0 and at most r_1 and r_2, respectively, i.e.,

$$\overrightarrow{m}_{[0,r_1]}(x) = \begin{bmatrix} 1 \\ x(t) \\ \vdots \\ x^{r_1}(t) \end{bmatrix}, \quad \overrightarrow{m}_{[0,r_1]}(u) = \begin{bmatrix} 1 \\ u(t) \\ \vdots \\ u^{r_2}(t) \end{bmatrix} \tag{15}$$

and, p_x, p_u denote two vectors that need to be identified using the available data. Note that $\overrightarrow{m}_{[0,r_1]}(x)$ and $\overrightarrow{m}_{[0,r_2]}(u)$ are concatenated polynomial vectors for $x \in \mathbb{R}^n$ and $u \in \mathbb{R}^m$ and $\mathscr{O}_t(\cdot,\cdot)$ in (14) is a linear function parametrized by a set of coefficients $\Xi = \left[P_x^{\mathrm{T}}, P_u^{\mathrm{T}}\right]^{\mathrm{T}} \in \mathbb{R}^l$ with $l = (r_1+1)+(r_2+1)$; that is, $\mathscr{O}_t(\cdot,\cdot)$ is a polynomial vector consisting of the (r_1+r_2+2) vectors. Then, writing in a compact form for (14) results in

$$\mathscr{O}_t(x(t),u(t)) = \Xi^{\mathrm{T}} \begin{bmatrix} \overrightarrow{m}_{[0,r_1]}(x(t)) \\ \overrightarrow{m}_{[0,r_2]}(u(t)) \end{bmatrix}. \tag{16}$$

Next, using the input data $\{u(t)\}_{t=0}^{k}$ in set $\mathbb{I}$ and the data $\{x(t)\}_{t=0}^{k}$ in set $\mathbb{O}$, we can construct the data

$$y(t) = x(t+1) - (Ax(t) + Bu(t)) \tag{17}$$

and then, form $\overrightarrow{m}_{[0,r_1]}(x)$ and $\overrightarrow{m}_{[0,r_1]}(u)$ for $t = 1,2,\ldots,k$. Then given two integers r_1 and r_2, using the least-squares method, we can optimize the parameter Ξ by solving

$$\hat{\Xi} = \arg\min_{\Xi} \sum_{k=0}^{t} \left\| \left(y(k) - \Xi^{\mathrm{T}} \begin{bmatrix} \overrightarrow{m}_{[0,r_1]}(x(t)) \\ \overrightarrow{m}_{[0,r_2]}(u(t)) \end{bmatrix} \right) \right\|^2 \tag{18}$$

Note that the $\mathscr{O}_t(x(t),u(t))$ given by (16) is linear in the coefficients Ξ, where $\overrightarrow{m}_{[0,r_1]}(x)$ and $\overrightarrow{m}_{[0,r_1]}(u)$ are two sets of polynomial vectors. This indicates that the least-squares optimization (18) has linear computational complexity, which greatly simplifies the computation load.

We highlight that the data-enhanced learning function given by (14) has two different meanings. The first is that (14) allows for corrections to be made to the nominal model given by (5): the second element of (15) modifies the A, B matrices of the nominal model; the remainder of (15) produces a more accurate model than the nominal one. The second is that the coefficients of (14) are characterized as unique optimizers of the least-squares problem (18). Using data-enhanced learning compensation given by (14) for the nominal model, it provides specific predictions of future behaviors, resulting in more accurate inputs and outputs for minimization of the performance function in solving (12).

3.4 Summary of the Main Results

Our proposed method describing the data-enhanced learning compensation for tube MPC is summarized in Algorithm 1.

Algorithm 1: Data-enhanced learning predictive controller

Data: Collect histrotical input and output data
Input: r_1, r_2
Output: $\zeta(t)$ for every t
$k \leftarrow t$;
while $k \geq \max(r_1, r_2)$ **do**
  if $t \geq 0$ **then**
    Form $\overrightarrow{m}_{[0,r_1]}(x)$ and $\overrightarrow{m}_{[0,r_1]}(u)$ given by (15);
    Solve (18) to obtain an estimate of Ξ;
    Solve (12) to obtain $\zeta(t+k)$, $k = 0,1,\ldots,N-1$;
  end
  Apply $\tilde{u}(t) = K\bar{x}(t) + \zeta(t)$ to the system;
  $t \leftarrow t+1$;
end

Note that the data-enhanced learning compensation method for MPC does not need any *a priori* assumptions for the nonlinear dynamic behavior $f(\cdot,\cdot)$ or the nonlinear term $g(\cdot,\cdot)$ in (10) after extracting a dominant linear behavior. This implies a distinctive feature of our design: Algorithm 1 is flexible enough to handle a broad range of nonlinear chemical processes: from a partially known system to an unknown system, identifying the system from effective data as a dominant linear plant. Using the previous data, it enables us to incorporate non-traditional models of adaptation into the prediction model, resulting in a lower cost and higher performance.

Due to the fact that our method retains the feasibility and constraint satisfaction of the tube MPC given by (9), we can design the data-enhanced learning function without having to worry about stability properties or the 'persistent excitation' requirement used in Marafioti et al. (2014). For the true plant, as long as (14) can be computed with available data, the purposed Algorithm 1 can be executed. In this sense, our purposed Algorithm 1 illustrates a clear separation between robustness and performance.

4. CASE STUDIES

In this section, we revisit the motivating example to demonstrate the properties of the developed controllers and the superior performance of Algorithm 1. To that end, using a sampling time of 0.1 min, we obtain the discrete-time state-space model with the form of (5) with matrices A, B given by

$$A = \begin{bmatrix} 0.8906 & -0.3419 \\ 0.0090 & 0.9067 \end{bmatrix}, \quad B = \begin{bmatrix} -0.0337 \\ 0.1811 \end{bmatrix}.$$

Note that the pair (A,B) is controllable. Using (2), we can write the constraints given by (3) in the following form

$$\mathscr{X} = \left\{ x(t) = \begin{bmatrix} x_1(t) \\ x_2(t) \end{bmatrix} : \begin{Bmatrix} -0.5 < x_1(t) < 0.5 \\ -0.4 < x_2(t) < 0.4 \end{Bmatrix} \right\} \tag{19a}$$

$$\mathscr{U} = \{ u(t) : -0.8 < u(t) < 0.8 \} \tag{19b}$$

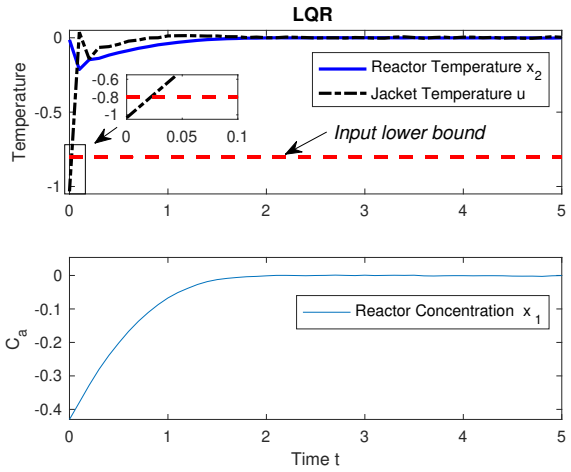

Fig. 2. Performance under the LQR controller given by (7).

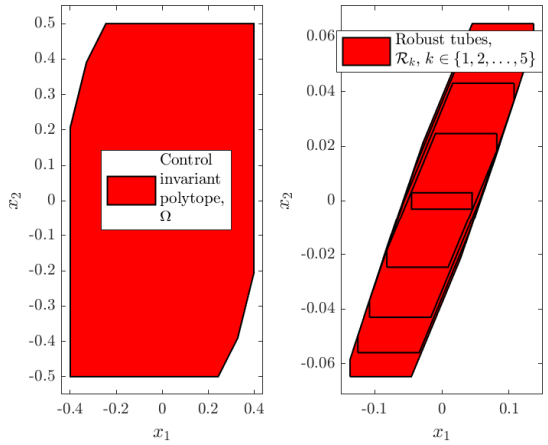

Fig. 3. The control invariant set Ω and the robust tubes $\mathscr{R}_k$.

The initial values of the CSTR system are set as $T(0) = 320$ K and $c_A(0) = 0.5$ mol/L, which corresponds to $x(0) = [-0.4300, -0.0138]$. Next, to render the states to the operating point given by (2), we will now check the system performance under all the controllers developed in Section 3.

First, to apply the LQR controller to the system, we set the weighting matrices as $Q = P = \mathrm{diag}([10\ 10])$ and $R = 0.1$, respectively. Thus, we obtain the feedback control gain K as

$$K = [2.5529\ \ -4.7132].$$

The system performance under the LQR controller given by (7) is depicted in Fig. 2. Note that the LQR controller can stabilize the CSTR system. However, it violates the constraint of the input lower bound given by (19b) at the beginning. If the constraints are violated at any time t, serious consequences may ensue, for example, physical components may be damaged or saturation may cause a loss of closed-loop stability. Fig. 2 indicates that the LQR cannot handle the constraints.

Next, to apply the tube-based MPC to the system, we set the control horizon as $N = 5$ and construct the control invariant set Ω and the robust tubes $\mathscr{R}_k$ given by (8), which are both illustrated in Fig. 3. Then we solve the OCP given by (9) at each sampling time t. The system performance under the tube-based MPC is depicted in Fig. 4. As shown in Fig. 4, the tube-based MPC can render the system state to the operating point without violating the constraints given by (19).

Then, we apply our proposed Algorithm 1 to the system. First, we set $r_1 = 2$ and $r_2 = 2$ for (15). Then we use Algorithm 1 to control the CSTR system given by (4) at each sampling time t. The system performance under Algorithm 1 is shown in Fig. 5. From the comparison of Figs. 5 and 4, we see that Algorithm 1 can significantly accelerate the convergence rate of tube-based MPC, while also satisfying all the constraints given by (19).

Finally, to illustrate the superior performance of Algorithm 1, we compare the accumulated costs associated with the LQR, the tube-based MPC, and Algorithm 1, as shown in Fig. 6. Fig. 6 reveals that the accumulated cost for Algorithm 1 is less than that of the LQR and the tube-based MPC. This indicates that the data-enhanced learning compensation method can improve the control performance of linear predictive controllers.

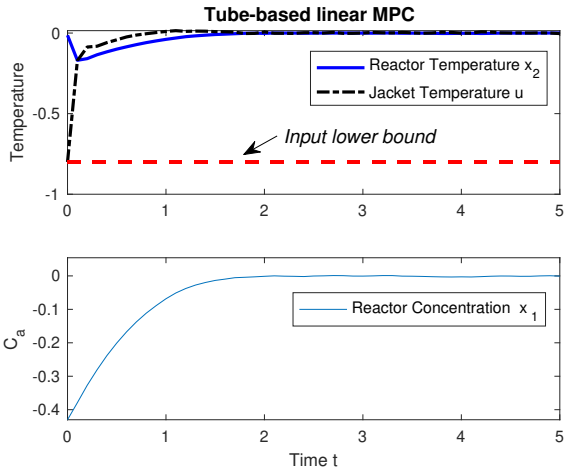

Fig. 4. Performance under the tube-based MPC given by (8).

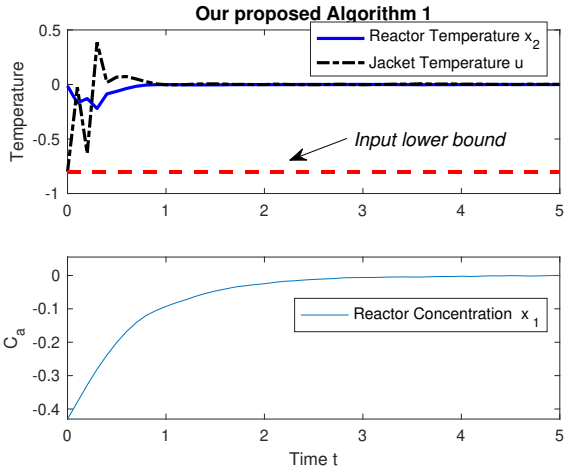

Fig. 5. Performance under our proposed Algorithm 1.

5. CONCLUSIONS

As chemical processes always have nonlinear dynamics and constraints, constrained optimization is a better method to control them. LQR and MPC have gained popularity because of their robustness and stability guarantees, but their formulations are typically LTI derivations of underlying system dynamics.

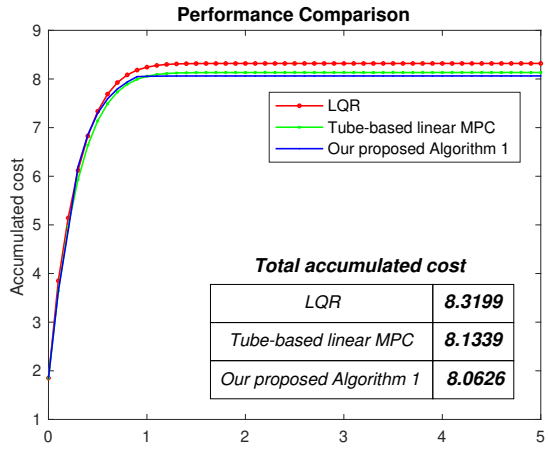

Fig. 6. System performance under our proposed Algorithm 1.

By incorporating statistics and machine learning techniques into the design process, this paper developed a data-enhanced learning compensation for closed loop performance improvement. Using this method, one can tune the prediction model used in tube-based MPC while ensuring the robustness and performance of the closed-loop system simultaneously. The method can be used for situations where engineering constraints must be satisfied by a system with dynamics that are unknown or with nonlinearities that make traditional control methods ineffective.

REFERENCES

Aswani, A., Gonzalez, H., Sastry, S.S., and Tomlin, C. (2013). Provably safe and robust learning-based model predictive control. *Automatica*, 49(5), 1216–1226.

Chisci, L., Rossiter, J.A., and Zappa, G. (2001). Systems with persistent disturbances: predictive control with restricted constraints. *Automatica*, 37(7), 1019–1028.

Edgar, T.F., Himmelblau, D.M., and Lasdon, L.S. (2001). *Optimization of Chemical Processes*. McGraw-Hill, New, York, NY.

Hewing, L., Wabersich, K.P., Menner, M., and Zeilinger, M.N. (2020). Learning-based model predictive control: Toward safe learning in control. *Annual Review of Control, Robotics, and Autonomous Systems*, 3, 269–296.

Lewis, F.L., Vrabie, D., and Syrmos, V.L. (2012). *Optimal Control*. John Wiley & Sons, Hoboken, NJ.

Lu, J., Cao, Z., Zhao, C., and Gao, F. (2019). 110th anniversary: An overview on learning-based model predictive control for batch processes. *Industrial & Engineering Chemistry Research*, 58(37), 17164–17173.

Marafioti, G., Bitmead, R.R., and Hovd, M. (2014). Persistently exciting model predictive control. *International Journal of Adaptive Control and Signal Processing*, 28(6), 536–552.

Mayne, D.Q. (2014). Model predictive control: Recent developments and future promise. *Automatica*, 50(12), 2967–2986.

Ogata, K. (2010). *Modern Control Engineering*. Prentice hall, Hoboken, NJ.

Olalla, C., Leyva, R., El Aroudi, A., and Queinnec, I. (2009). Robust LQR control for PWM converters: An LMI approach. *IEEE Transactions on Industrial Electronics*, 56(7), 2548–2558.

Prett, D.M. and García, C.E. (2013). *Fundamental Process Control: Butterworths Series in Chemical Engineering*. Butterworth-Heinemann, Stoneham, MA.

Qin, S.J. and Badgwell, T.A. (2003). A survey of industrial model predictive control technology. *Control Engineering Practice*, 11(7), 733–764.

Qin, S.J. and Dong, Y. (2020). On data science for process systems modeling, control and operations. *IFAC-PapersOnLine*, 53(2), 11325–11331.

Rakovic, S.V., Kerrigan, E.C., Kouramas, K.I., and Mayne, D.Q. (2005). Invariant approximations of the minimal robust positively invariant set. *IEEE Transactions on Automatic Control*, 50(3), 406–410.

Rakovic, S.V., Kouvaritakis, B., Cannon, M., Panos, C., and Findeisen, R. (2012). Parameterized tube model predictive control. *IEEE Transactions on Automatic Control*, 57(11), 2746–2761.

Seborg, D.E., Mellichamp, D.A., Edgar, T.F., and Doyle III, F.J. (2010). *Process Dynamics and Control*. John Wiley & Sons, New York, NY.

Wu, Z., Rincon, D., Luo, J., and Christofides, P.D. (2021). Machine learning modeling and predictive control of nonlinear processes using noisy data. *AIChE Journal*, 67(4), e17164.

Yang, Y., Chen, X., Lu, N., and Gao, F. (2016). *Injection Molding Process Control, Monitoring, and Optimization*. Hanser Publications, Cincinnati, Ohio, USA.

Zhou, H. (2012). *Computer Modeling for Injection Molding: Simulation, Optimization, and Control*. John Wiley & Sons, Hoboken, NJ.

Zhou, Y., Gao, K., Tang, X., Hu, H., Li, D., and Gao, F. (2022a). Conic input mapping design of constrained optimal iterative learning controller for uncertain systems. *IEEE Transactions on Cybernetics*, 1–13. doi:10.1109/TCYB.2022.3155754.

Zhou, Y., Li, D., and Gao, F. (2022b). Conic iterative learning control using distinct data for constrained systems with state-dependent uncertainty. *IEEE Transactions on Industrial Informatics*, 18(5), 3095–3104.

Zhou, Y., Li, D., Xi, Y., and Gan, Z. (2020). Synthesis of model predictive control based on data-driven learning. *Science China Information Sciences*, 63, 1–3.

Zhou, Y., Li, D., Xi, Y., and Gao, F. (2022c). Event-triggered distributed robust model predictive control for a class of nonlinear interconnected systems. *Automatica*, 136, 110039.

Appendix A. PARAMETERS OF THE CSTR SYSTEM

Table A.1. Parameters of the CSTR

Parameter	Explanation	Nominal value	Units
F_i	Inlet flow rate	100	L/min
c_{Ai}	Feed concentration	1	mol/L
T_i	Feed temperature	350	K
V	Volume of CSTR	100	L
k_0	Pre-exponential factor	7.2×10^{10}	min^{-1}
E/R	E/R = Activation energy	8750	K
UA	Heat transfer constant	5×10^4	J/min·K
ρ	Density of A-B mixture	1000	g/L
C_p	Heat capacity of A-B mixture	0.239	J/g·K
ΔH_R	Heat of reaction for $A \to B$	-5×10^4	J/mol